J Solid State Electrochem (2009) 13:353–363
DOI 10.1007/s10008-008-0553-z

ORIGINAL PAPER

# Electrochemical characterization of 2, 2′-[1, 2-ethanediylbis (nitriloethylidyne)]-bis-hydroquinone-carbon nanotube paste electrode and its application to simultaneous voltammetric determination of ascorbic acid and uric acid

**Hadi Beitollahi · Mohammad Mazloum Ardakani · Hossein Naeimi · Bahram Ganjipour**

Received: 1 January 2008 / Accepted: 17 March 2008 / Published online: 6 May 2008


**Abstract** The preparation and electrochemical characterization of a carbon nanotube paste electrode modified with 2,2′-[1,2-ethanediylbis (nitriloethylidyne)]-bis-hydroquinone, referred to as EBNBH, was investigated. The EBNBH carbon nanotube paste electrode (EBNBHCNPE) displayed one pair of reversible peaks at $E_{pa}$=0.18 V and $E_{pc}$=0.115 V vs Ag/AgCl. Half wave potential ($E_{1/2}$) and $\Delta E_p$ were 0.148 and 0.065 V vs Ag/AgCl, respectively. The electrocatalytic oxidation of ascorbic acid (AA) has been studied on EBNBHCNPE, using cyclic voltammetry, differential pulse voltammetry and chronoamperometry techniques. It has been shown that the oxidation of AA occurs at a potential where oxidation is not observed at the unmodified carbon paste electrode. The heterogeneous rate constant for oxidation of AA at the EBNBHCNPE was also determined and found to be about $1.07\times10^{-3}$ cm $s^{-1}$. The diffusion coefficient of AA was also estimated as $5.66\times10^{-6}$ $cm^2$ $s^{-1}$ for the experimental conditions, using chronoamperometry. Also, this modified electrode presented the property of electrocatalysing the oxidation of AA and uric acid (UA) at 0.18 and 0.35 V vs Ag/AgCl, respectively. The separations of anodic peak potentials of AA and UA reached 0.17 V. Using differential pulse voltammetry, the calibration curves for AA and UA were obtained over the range of 0.1–800 μM and 20–700 μM, respectively. With good selectivity and sensitivity, the present method provides a simple method for selective detection of AA and UA in biological samples.

**Keywords** EBNBH · Ascorbic acid · Carbon nanotube paste electrode · Electrocatalytic oxidation · Voltammetry · Chronoamperometry

H. Beitollahi · M. Mazloum Ardakani (✉)
Department of Chemistry, Faculty of Science, Yazd University, Yazd, Iran
e-mail: mazloum@yazduni.ac.ir

H. Naeimi
Department of Chemistry, Faculty of Science, Kashan University, Kashan, Iran

B. Ganjipour
Institute of Nanotechnology, Kashan University, Kashan, Iran

## Introduction

Electrochemical methods traditionally have found important applications in sample analysis and in organic and inorganic synthesis. The electrode surface itself can be a powerful tool in such applications [1]. Apart from the conventional electrodes such as Au, Hg, and Pt, carbon is a preferred substrate in electroanalytical studies [2]. Biological fluids are best determined at modified carbon electrodes [3], and also at modified carbon paste electrodes [4]. The overpotential phenomena make most of the clinically important compounds difficult to analyze at conventional electrodes which is promoted by incorporating redox mediators by various methods [5]. There are four principle enhancement techniques for voltammetric and amprometric electrodes, namely selective preconcentration, permselectivity, selective recognition and electrocatalysis [6].

The base of modified carbon pastes is usually a mixture of powdered graphite and nonelectrolytic binder. Another constituent in the mixture is then a modifier itself. The main reason to modify an electrode is to obtain qualitatively new

sensor with desired, often predefined properties. Carbon pastes undoubtedly represent one of the most convenient materials for the preparation of modified electrodes.

Redox materials are small electroactive compounds that effectively shuttle electrons between the analyte and the electrode. Several types of chemically modified electrodes (CMEs) have been designed and characterized for electrocatalysis of biological fluids particularly for vitamins such as ascorbic acid.

Since their discovery in 1991 [7], carbon nanotubes (CNTs) have been one of the most actively studied materials because of their unique structure and extraordinary physical properties and industrial application possibilities such as hydrogen storage material [8], capacitors [9], battery electrode [10], and field emission displays [11]. In this regard, it is necessary to scale up the growth of carbon nanotubes by improving the activity of catalysts and the environment of growth by investigating the growth characteristics appropriately and elaborately.

Ascorbic acid (AA) is known for its reductive properties and for its use on a wide scale as an antioxidant agent in food and drinks; it is also important for therapeutic purposes and biological metabolism. Therefore, recent advances in the food and pharmaceutical industries and a need for nutritional assessment have necessitated the development of a selective, simple, and accurate method to determine AA [12, 13]. Due to its selectivity and sensitivity, an electrochemical method to determine AA has been a subject of considerable interest. A variety of examples of the electrochemical determination of AA have been proposed. These include a glassy carbon electrode (GCE) and a carbon paste electrode with complexes and organic compounds, such as, Naphthol green B doped in polypyrrole film [14], cobalt phthalocyanine nanoparticles [15], poly(caffeic acid) [16], octacyanomolybdate-doped-poly(4-vinylpyridine) [17], ferrocene and its derivatives [18–20], vanadium oxide polypropylene carbonate [21], ruthenium oxide [22] and polyaniline film [23].

Thus, in this paper, we described initially the preparation and suitability of a 2, 2′-[1, 2-Ethanediylbis (nitriloethylidyne)]-bis-hydroquinone (Scheme 1) modified carbon nanotube paste electrode (EBNBHCNPE) as a new electrocatalyst in the electrocatalysis and determination of AA in an aqueous buffer solution, then we evaluated the analytical performance of the modified electrode in quantification of AA in the presence of UA. Finally, in order to demonstrate the catalytic ability of this modified electrode in the electrooxidation of AA in real samples, we examined this method for the voltammetric determination of AA in pharmaceutical preparation.

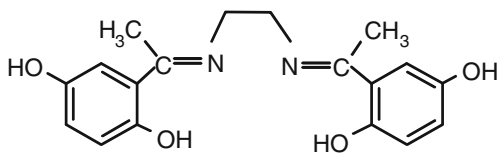


**Scheme 1** Structure of 2, 2′-[1, 2-Ethanediylbis (nitriloethylidyne)]-bis-hydroquinone

## Experimental

### Apparatus and chemicals

Voltammetric measurements were carried out using a computerized potentiostat/galvanostat Autolab model PGSTAT30 (EcoChemie B. V.A). The experimental were controlled with general purpose electrochemical system (GPES) software. All electrochemical studies were performed at 25±1°C with a three-electrode assembly included a 50-ml glass cell, a Ag/AgCl electrode as reference electrode, a platinum wire counter electrode, and the working electrode was a EBNBHCNPE. All potentials were measured and reported vs the Ag/AgCl reference electrode. A Metrohm 781 pH/ion meter was also used for pH measurements.

All solutions were freshly prepared with double-distilled water. Ascorbic acid, uric acid, and reagents were of analytical grade from Merck. Graphite fine powder (Merck) and paraffin oil (DC 350, Merck, density=0.88 g $cm^{-3}$) were used as binding agents for the graphite pastes. Before use, flasks and containers were soaked in 6 M $HNO_3$ for at least 24 h, then rinsed with double-distilled water. The buffer solutions were prepared from orthophosphoric acid and its salts in the pH range 2.0–11.0. Potassium chloride 0.1 M was as supporting electrolyte in all experiments.

### Synthesis of 2, 2′-[1, 2-ethanediylbis (nitriloethylidyne)]-bis-hydroquinone

To a mixture of 2,5-dihydroxyacetophenone (0.3 g, 2 mmol) in methanol, 1, 2-diaminoethane (0.06 g, 1 mmol) was added by stirring for 60 min. Progress of the reaction was monitored by TLC. After reaction completion, a yellow substance was precipitated, then filtered off and washed with cold methanol. The crude product was recrystallized in methanol, and the 2,2′-[1,2-ethanediylbis (nitriloethylidyne)]-bis-hydroquinone was obtained as yellow crystals in~ 95% yield.

*2,2′ -[1,2-ethanediylbis (nitriloethylidyne)]-bis-hydroquinone*: yellow solid m.p. 284–287°C; IR (KBr)/υ($cm^{-1}$) 3100–3300 (br, OH), 2990, 2800, 1608(s, C = N),1390, 1550(s, Ar, C = C), 1250(s, C-O), 1300(s), 1200(s), 850, 800(s), 500(w); $^1$H NMR (400 MHz/ DMSO)/ δ ppm: 2.1 (s, 6 H, 2 $CH_3$), 3.67(s, 4 H, 2 $CH_2$), 6.4(d, 2 H, Ar), 6.54(d of d, 2 H, Ar), 6.81(d of d, 2 H, Ar), 8.6(br, 2 H, 2 OH),

14.7(s, 2 H, 2 OH); $^{13}$C NMR (100 MHz/DMSO)/δ ppm: 16.4, 51.7, 115.4, 119.4, 120.8, 121.5, 149.8, 156.4, 172.0.

### Synthesis of carbon nanotube

Double wall nanotubes (DWNTs) produced by the catalyst chemical vapor deposition method (CVD) and arc discharge methods are purified using an acid treatment [24, 25]. Recently, two different approaches for the purification of single wall nanotubes (SWNTs) synthesized over zeolite using CVD have been reported [26, 27]. The treatment involving HF is reported to be more effective in removing both zeolite and metal particles [27]. During an industrial scale purification process of CVD grown nanotubes the use of common chemicals such as NaOH and HCl is recommended instead of harmful HF. In this present work, we used oxidation and acid treatment of the carbon nanotubes to remove carbonaceous impurities or to clear the metal surface. In this study all samples are exposed to hot air flow at 450°C for 1 h. After which, acid treatment in 30% wt HCl for 24 h is used and finally samples are rinsed with double-distilled water.

The nanotubes were grown by the chemical vapor deposition method. Several transition metal catalysts have been shown to be active for generation of carbon nanotubes [24, 25]. Among the various formulations that we have investigated, Co–Fe silica (MCM41-96) catalyst, containing 2.5 wt% total metals and a Co/Fe molar ratio of 1:1 exhibited high selectivity towards DWNT. This catalyst was prepared by methanolic solutions of cobalt acetate and iron acetate, followed by activating at 300°C for 30 min under a 500 ml/min of Ar flow rate in a quartz tube [28]. For the production of nanotubes, 100–500 mg of activated catalyst was placed in a horizontal quartz tubular reactor, heated in $H_2$ up to 500°C, and then in He to 900°C. The quartz tube is pumped out during the Combustion (Catalytic) Chemical Vapor Deposition CCVD process. Methane was introduced at this temperature for 20 min and at a flow rate of 100 sccm for the production of nanotubes. After the CCVD synthesis, the nanotube material is cooled under He atmosphere. The diameter, length, purity and surface area of DWCNTs was ~2.5 nm (outer diameter of DWCNTs is in the range of 1.52–3.54 nm), 5–15 μm, 90%, 97 $m^2/g$ (roughly), respectively.

### Preparation of the EBNBH carbon nanotube paste electrode

A 0.01 g of EBNBH was dissolved in $CH_3Cl$ and hand mixed with 89-times its weight of graphite powder and 10-times its weight of carbon nanotube with a mortar and pestle. The solvent was evaporated by stirring. Paraffin (Dc 350, Merck) were added to the above mixture using a 5-ml syringe and mixed for 20 min until a uniformly-wetted paste was obtained. The paste was then packed into the end of a glass tube (ca. 2 mm i.d. and 10 cm long). Electrical contact was made by pushing a copper wire down the glass tube into the back of the mixture. When necessary, a new surface was obtained by pushing an excess of paste out of the tube and polishing it on a weighing paper. Also, a modified carbon paste disk served as the working electrode for RDE experiments. The body of the carbon paste-working electrode was a Teflon rod with a hole (2 mm diameter, 5 mm deep) bored at one end for electrode filling. Contact was made with a platinum wire through the center of the rod, which screwed to the RDE device.

Unmodified carbon paste electrode was prepared in the same way without adding EBNBH and carbon nanotube to the mixture and was used for comparison purposes.

## Results and discussion

The EBNBH complex is insoluble in aqueous solutions; it can be used into the carbon paste without leaching out from the electrode surface, thus leading to a chemically modified electrode that may be very stable. The electrochemical behavior of the EBNBH modified electrode was investigated. Figure 1 shows the cyclic voltammograms for the modified electrode at different scan rates in 0.1 M phosphate buffer with pH 7.0. As can be seen, the cyclic voltammogram exhibits an anodic peak at a forward scan of the potential related to the oxidation of the EBNBH to quinone form of EBNBQ. Whereas at a reverse scan of the potential, a cathodic peak appears related to the reduction of quinone form EBNBQ to EBNBH. A pair of reversible peaks observed at $E_{pa}$=0.180 V and $E_{pc}$=0.115 V vs Ag/AgCl. Half wave potential ($E_{1/2}$) and $\Delta E_p$ were 0.148 V vs Ag/AgCl and 0.065 V, respectively. As can be seen, the peak separation potential, $\Delta E_p$ (=$E_{pa}$ – $E_{pc}$), is greater than the (59/n) mV expected for a reversible system. This result suggests that an EBNBH/EBNBQ redox couple in EBNBHCNPE shows a quasi reversible behavior in an aqueous medium.

The representative cyclic voltammograms obtained for the EBNBHCNPE are shown in Fig. 1 for various scan rates (10–1000 mV $s^{-1}$). Inset A of Fig. 1 shows anodic and cathodic peak currents ($I_p$) values were linearity dependent on υ at scan rates 10–1000 mV $s^{-1}$. A linear correlation was obtained between peak currents and the scan rate indicate that the nature of redox process is diffusionless controlled. Insets B and C of Fig. 1 show the magnitudes of peak potentials ($E_{pa}$ and $E_{pc}$) as a function of the potential scan rate.

Laviron derived general expressions for the linear potential sweep voltammetric response for the case of

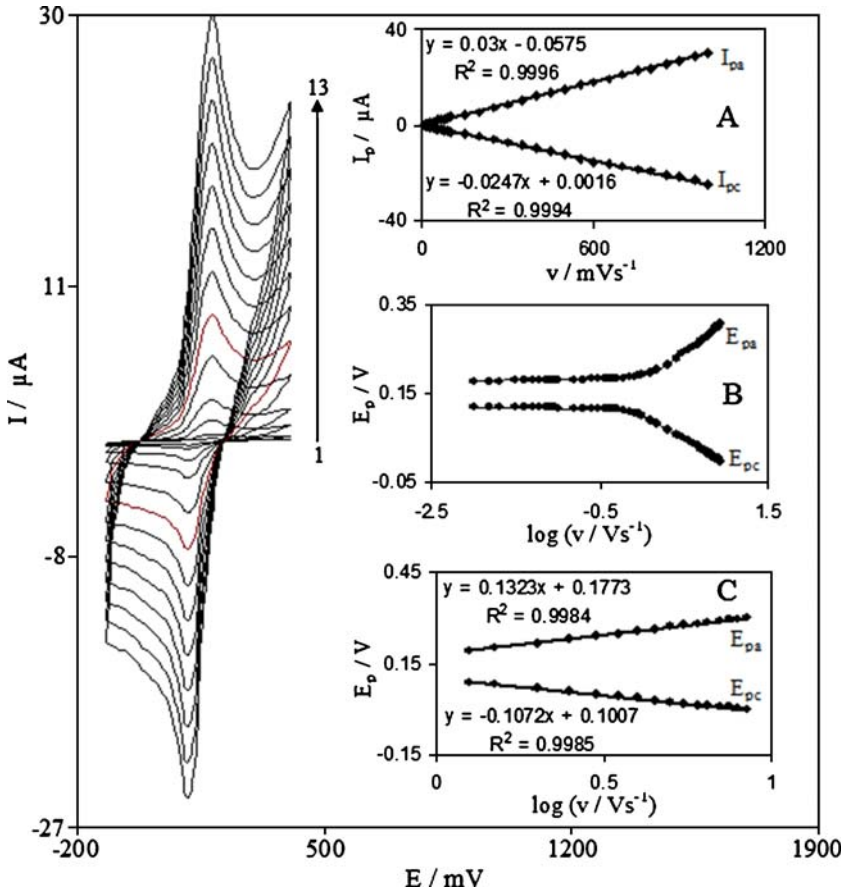


**Fig. 1** Cyclic voltammograms of EBNBHCNPE in 0.1 M phosphate buffer (pH 7.0), at various scan rates: the numbers 1–13 correspond to 10, 20, 50, 100, 200, 300, 400, 500, 600, 700, 800, 900 and 1000 $mVs^{-1}$ scan rates, respectively. Insets: *A* variations of Ip versus scan rates; *B* variation of Ep versus the logarithm of the scan rate; *C* magnification of the same plot for high scan rates

surface-confined electroactive species with a concentration small enough [29]:

$$E_{pc} = E^{\circ} + A\ln[1-\alpha/m] \tag{1}$$

$$E_{\mathrm{pa}} = E^{\circ} + \mathrm{B}\ln[\alpha/\mathrm{m}] \tag{2}$$

For $E_{\mathrm{pa}} - E_{\mathrm{pc}} = \Delta E_{\mathrm{p}} > 200/\mathrm{n\,mV}$ :

$$\log \mathrm{k_s} = \alpha\log(1-\alpha) + (1-\alpha)\log\alpha - \log(\mathrm{RT/nFv}) - \alpha(1-\alpha)\mathrm{nF}\Delta\mathrm{E_p}/2.3\mathrm{RT} \tag{3}$$

where $A$ = RT/ (1-α) nF, $B$ = RT/αnF and $m$ = (RT/F) ($k_s/n_\alpha$).

From these expressions, it is possible to determine the transfer coefficient (α) by measuring the variation of the peak potentials with scan rate (ν) as well as the apparent charge transfer rate constant ($k_s$) for electron transfer between the electrode and the surface confined layer. A plot of $E_p = f(\log \nu)$ yields two straight lines with slopes equal to 2.3RT/αnF and 2.3RT/(1-α) nF for the anodic and cathodic peaks, respectively. We have found that for scan rates above 1,000 $mVs^{-1}$, the values of $\Delta E = (E_p\text{-}E^{\circ\prime})$ were proportional to the logarithm of scan rate as was indicated by Laviron. The plots are shown in inset C of Fig. 1. Using such plot and Eq. 3, the values of α and $k_s$ were 0.55 and 8.89 $s^{-1}$, respectively, for the EBNBHCNPE in the presence of 0.1 M phosphate buffer.

An approximate estimate of the surface coverage of the electrode was made by adopting the method used by Bard [30]. The values for the surface concentration of EBNBH (Γ), given in mol $cm^{-2}$ were obtained from the integrated charges (Q) of the anodic peak as follows:

$$\Gamma_{\mathrm{EBNBH}} = \mathrm{Q/nFA} \tag{4}$$

where $Q$ is the charge from the area under the EBNBH anodic peak corrected for the baseline, and could be easily observed from cyclic voltammograms; $n$ is the number of electrons exchanged per reactant molecule. The calculated surface concentration of EBNBH is $2.51\times10^{-10}$ mol $cm^{-2}$ for $n$=2.

## Effect of pH on the EBNBHCNPE

The electrochemical behavior of the EBNBHCNPE was studied over a pH range between 2.0 and 11.0 at scan rate

50 mV $s^{-1}$. The obtained result shows that the variation in the pH has effect on the half-wave potential of the redox system. The EBNBH to quinone form of EBNBQ process is dependent on the pH.

The formal potential (E°′) of the surface redox couple were pH dependent. The results showed that the slope (E°′/pH) is 59.6 mV/pH unit over a pH range from 2.0 to 7.0. This slope was close to the Nernstian value of 59.2 mV for a two electron, two proton process. However, such a process can be considered as a simple reaction with two successive one-electron exchanges as indicated by Laviron for the conditions at which the transfer coefficients of the electrochemical reactions are about 0.5 and protonations are at equilibrium. Change of the slope for pH value above 7.0 can be described to the deprotonation of the confined EBNBH. The value obtained for the $pK_a$ of surface confined EBNBH was 7.1. The slope of the 29.9 mV/pH unit was anticipated for pH values more than 7.0, which is very close to the Nernstian value of 29.6 mV for a two-electron, one-proton process.

## Electrocatalytic oxidation of ascorbic acid

Figure 2 depicts the cyclic voltammetric responses from the electrochemical oxidation of 1.0 mM AA at EBNBHCNPE (curve f), EBNBHCPE (curve e), CNPE (curve d), bare CPE (curve b). As can be seen, the anodic peak potential

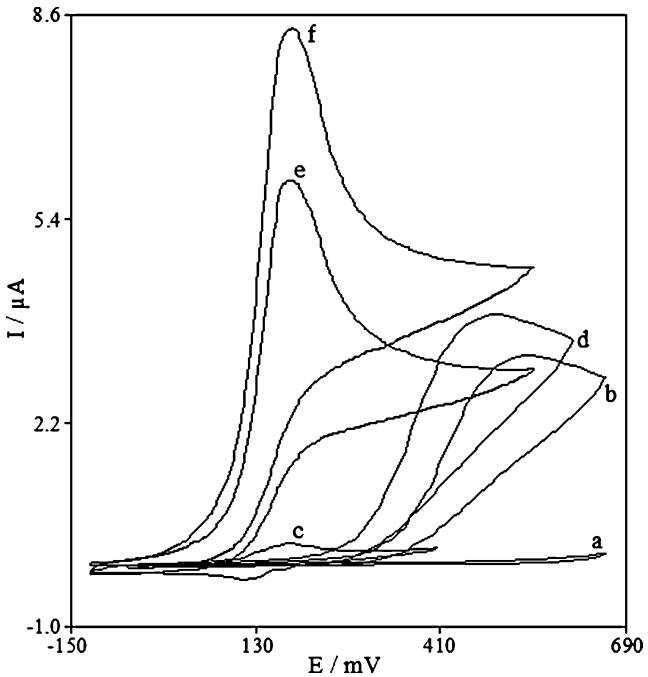


**Fig. 2** Cyclic voltammograms of (*a*) CPE in 0.1 M phosphate buffer solution (pH 7.0) at scan rate 10 mV $s^{-1}$ and (*b*) as (*a*)+1 mM AA; (*c*) as (*a*) and (*d*) as (*b*) at the surface of EBNBHCNPE and EBNBHCPE respectively. Also, (*e*) and (*f*) as (*b*) at the surface of EBNBHCPE and EBNBHCNPE respectively

for the oxidation of AA at EBNBHCNPE (curve f) and EBNBHCPE (curve e) is about 180 mV, while at the CNPE (curve d) peak potential is about 500 mV, and at the bare CPE peak potential is about 560 mV of AA (curve b).

From these results it is concluded that the best electrocatalytic effect for AA oxidation is observed at EBNBHCNPE (curve f). For example, the results are shown that the peak potential of AA oxidation at EBNBHCNPE (curve f) shifted by about 320 and 380 mV toward the negative values compared with that at a CNPE (curve d) and bare CPE (curve b), respectively. This value is comparable with values reported by other research groups for electrocatalytic oxidation of ascorbic acid at the surface of chemically modified electrodes by other mediators (see Table 1).

Similarly, when we compared the oxidation of AA at the EBNBHCPE (curve e) and EBNBHCNPE (curve f); there is a dramatic enhancement of the anodic peak current at EBNBHCNPE relative to the value obtained at the EBNBHCPE. In other words, the data obtained clearly show that the combination of carbon nanotube and mediator (EBNBH) definitely improve the characteristics of AA oxidation. The EBNBHCNPE in 0.1 M phosphate buffer (pH 7.0), without AA in solution, exhibits a well-behaved redox reaction (curve c) upon the addition of 1.0 mM AA, there is a dramatic enhancement of the anodic peak current (curve f), which indicates a strong electrocatalytic effect. The reaction scheme would probably via following mechanistic steps, which AA can be oxidized by EBNBQ produced in the surface of electrode:

$$\mathrm{EBNBH} \rightarrow \mathrm{EBNBQ} + 2\mathrm{H}^{+} + 2\mathrm{e} : \mathrm{E}$$

$$\mathrm{EBNBQ} + (\mathrm{AA})_{\mathrm{red}} \rightarrow \mathrm{EBNBH} + (\mathrm{AA})_{\mathrm{ox}} : \mathrm{C}$$

The effect of the potential scan rate on the electrocatalytic properties of EBNBHCNPE in 0.1 M phosphate buffer solution containing 1 mM ascorbic acid was studied. Figure 3 shows the cyclic voltammograms of a EBNBHCNPE at various scan rates obtained in 0.1 M phosphate buffer solution (pH 7.0) containing 1 mM AA. The anodic oxidation current of AA is proportional to the square root of the scan rate (Fig. 3, inset A) indicating that at sufficiently positive potential the reaction is controlled by AA diffusion.

In order to obtain information on the rate-determining step, a Tafel slope, b, was determined using the following equation for a totally irreversible diffusion controlled process [31]:

$$E_{\mathrm{p}} = (\mathrm{b}/2)\log \mathrm{v} + \text{constant} \qquad (5)$$

On the basis of Eq. 5, the slope of $E_p$ vs log ν plot is b/2, where b indicates the Tafel slope. The slope of $E_p$ vs. log ν plot is $\partial E_p/\partial(\log \nu)$ and was found to be 44.701 mV in this work (Fig. 3, inset B), so $b = 2 \times 44.701 = 89.402$ mV. The

**Table 1** Comparison of the efficiency of some modified electrodes used in the electrocatalysis of ascorbic acid

| Substrate | Modifier | Method | pH | Peak potential shift (mV) | Scan rate (mV/s) | Limit of detection (M) | Dynamic range(M) | Reference |
|---|---|---|---|---|---|---|---|---|
| Platinum Electrode | Naphthol Green B | Voltammetry | 4.5 | 320 | 50 | $1.1\times10^{-4}$ | $2.4\times10^{-4}$–$2.5\times10^{-2}$ | 14 |
| Glassy Carbon Electrode | Cobalt phthalocyanine nanoparticles | Potentiometry | 7.0 | 190 | 200 | $1.0\times10^{-7}$ | $5.5\times10^{-7}$–$1.0\times10^{-2}$ | 15 |
| Carbon Paste Electrode | 2,7-Bis(ferrocenyl ethyl)fluoren-9-one | Voltammetry | 7.0 | 300 | 10 | $9.0\times10^{-6}$ | $3.1\times10^{-5}$–$3.3\times10^{-3}$ | 18 |
| Gold Electrode | Ferrocene | Voltammetry | 5.8 | _ | 50 | $2.0\times10^{-7}$ | $1.0\times10^{-6}$–$5.0\times10^{-4}$ | 19 |
| Glassy Carbon Electrode | Ruthenium Oxide | Voltammetry | 5.0 | 250 | 100 | $8.0\times10^{-5}$ | $8.8\times10^{-5}$–$2.32\times10^{-3}$ | 22 |
| Carbon Nanotube Paste Electrode | 2, 2′-[1, 2 Ethanediylbis (nitriloethylidyne)]-bis hydroquinone | Voltammetry | 7.0 | 380 | 10 | $7.5\times10^{-8}$ | $1.0\times10^{-7}$–$8.0\times10^{-4}$ | This work |

value of Tafel slope indicates that a one-electron transfer process is the rate limiting step assuming a transfer coefficient of $\alpha$ about 0.34. Figure 3, inset C, shows a Tafel plot that was drawn from data of the rising part of the current–voltage curve recorded at a scan rate of 10 $mVs^{-1}$. This part of voltammogram, known as Tafel region, is affected by electron transfer kinetics between substrate (AA) and surface confined EBNBH, assuming the deprotonation of substrate as a sufficiently fast step. In this condition, the number of electron involved in the rate determining step can be estimated from the slope of Tafel plot. A slope 89.56 $mVdecade^{-1}$ is obtained indicating a one electron transfer to be rate limiting assuming a transfer coefficient of $\alpha$=0.34.

## Chronoamperometric measurements

The chronoamperometry as well as the other electrochemical methods was employed for the investigation of electrode processes at chemically modified electrodes. Figure 4a shows chronoamperometric measurements of AA at EBNBHCNPE. This figure represents the current–

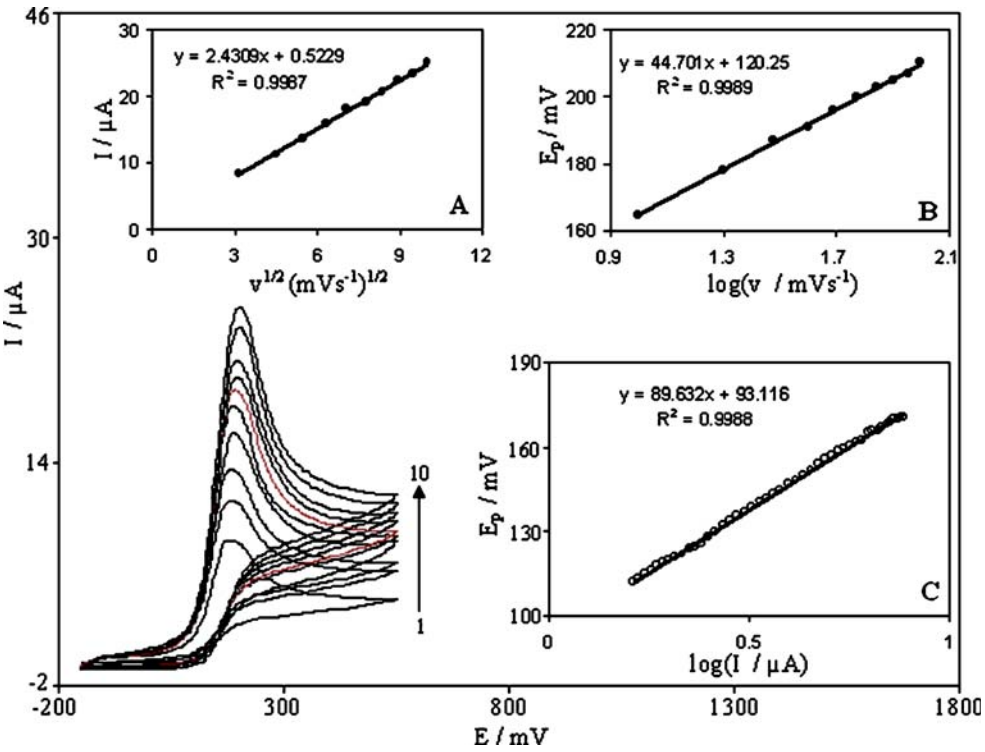


**Fig. 3** Cyclic voltammograms of the EBNBHCNPE in the presence of 1 mM AA at various scan rates; The numbers 1–10 correspond to 10, 20, 30, 40, 50, 60, 70, 80, 90, and 100 $mVs^{-1}$ scan rates, respectively Insets: *A* The variation of the anodic peak currents vs. $v^{1/2}$; *B* the variation of the anodic peak potential vs log *v*; *C* Tafel plot derived from the rising part of voltammogram recorded at a scan rate of 10 $mVs^{-1}$

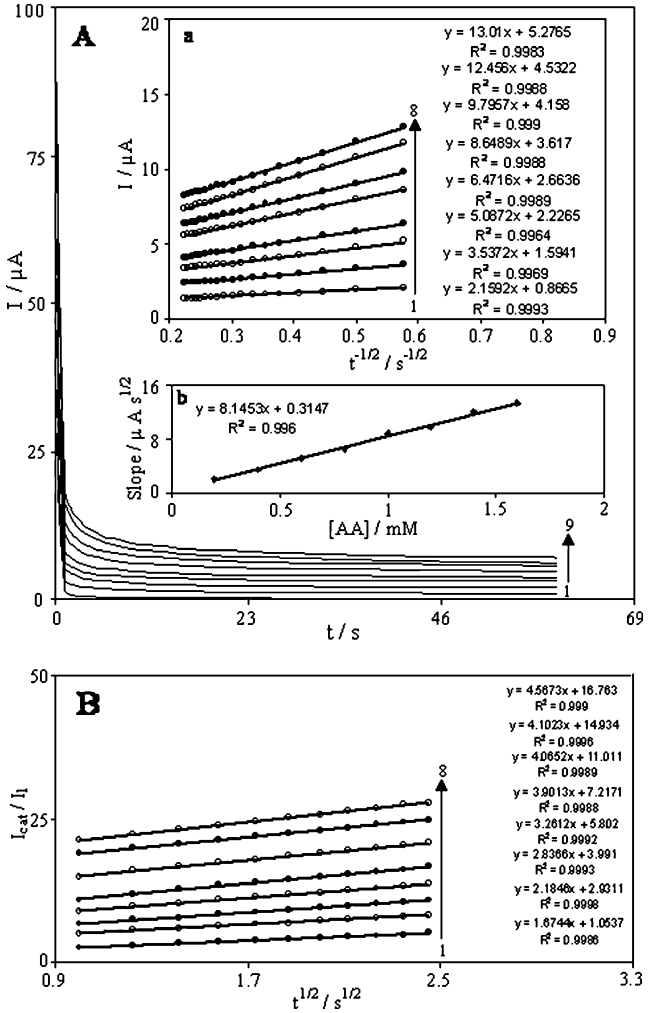


**Fig. 4** **a** Chronoamperograms obtained at EBNBHCNPE in 0.1 M phosphate buffer solution (pH 7.0) for different concentration of AA. The numbers 1–9 correspond to 0.0, 0.2, 0.4, 0.6, 0.8, 1.0, 1.2, 1.4, and 1.6 mM of AA. Insets: *A* Plots of I vs. $t^{-1/2}$ obtained from chronoamprograms 2–9 and **b** plot of the slope of the straight lines against the AA concentration. *B* Dependence of $I_{cat}/I_l$ on $t^{1/2}$ derived from the data of chronoamprograms shown in **a**

time profiles obtained by setting the working electrode potential at 600 mV for various concentrations of AA. In chronoamperometric studies, we have determined the diffusion coefficient of AA for an EBNBHCNPE. For an electroactive material (AA in this case) with a diffusion coefficient of D, the current for the electrochemical reaction (at a mass transport limited rate) is described by the Cottrell equation [30]:

$$I = nFAD^{1/2}C_b\pi^{-1/2}t^{-1/2} \quad (6)$$

Where $D$ and $C_b$ are the diffusion coefficient ($cm^2\ s^{-1}$) and the bulk concentration (mol $cm^{-3}$), respectively. Under diffusion control, a plot of I versus $t^{-1/2}$ will be linear, and from the slope the value of $D$ can be obtained. Figure 4a inset A shows the experimental plots with the best fits for different concentration of AA employed. The slopes of the resulting straight lines were plotted versus the AA concentration (Fig. 4a inset b). The mean value of the D was found to be $5.66\times10^{-6}$ $cm^2\ s^{-1}$.

Chronoamperometry can also be employed to evaluate the catalytic rate constant, $k$, for the reaction between AA and the EBNBHCNPE according to the method of Galus [32]:

$$I_C/I_L = \gamma^{1/2}\left[\pi^{1/2}\mathrm{erf}\left(\gamma^{1/2}\right) + \exp(-\gamma)/\gamma^{1/2}\right] \quad (7)$$

where $I_C$ is the catalytic current of AA at the EBNBHCNPE, $I_L$ the limited current in the absence of AA and $\gamma = kC_bt$ ($C_b$ is the bulk concentration of AA) is the argument of the error function. In the cases where γ exceeds 2, the error function is almost equal to 1, and therefore, the above equation can be reduced to:

$$I_C/I_L = \pi^{1/2}\gamma^{1/2} = \pi^{1/2}(kC_bt)^{1/2} \quad (8)$$

where $t$ is the time elapsed (s). The above equation can be used to calculate the rate constant of the catalytic process $k$. Based on the slope of the $I_C/I_L$ versus $t^{1/2}$ plot; $k$ can be obtained for a given AA concentration. Such plots obtained from the chronoamperograms in Fig. 4a are shown in Fig. 4b. From the values of the slopes an average value of k was found to be $k=4.27\times10^3$ $M^{-1}\ s^{-1}$. The value of $k$ explains as well as the sharp feature of the catalytic peak observed for catalytic oxidation of AA at the surface of EBNBHCNPE. Finally, the heterogeneous rate constant of catalytic reaction was calculated as $k'=1.07\times10^{-3}$ $cm\ s^{-1}$.

## Differential pulse voltammetry investigations

Since differential pulse voltammetry, DPV, has a much higher current sensitivity and better resolution than cyclic voltammetry, it was used to estimate the lower limit of detection of AA. In addition, the charging current contribution to the background current, which is a limiting factor in the analytical determination, is negligible in DPV mode. Figure 5 shows the DPVs obtained for the oxidation of different concentrations of AA at the EBNBHCNPE. The dependence of the peak current on the AA concentration is shown in inset A of Fig. 5. Insets B and C of this figure clearly show that the plot of peak current versus AA concentration is constituted of two linear segments with different slopes, corresponding to two different ranges of substrate concentration. The decrease of sensitivity (slope) in the second linear range (Fig. 5, inset C), is likely to be due to kinetic limitation. From the analysis of these data, we estimate that the lower limit of detection of AA is of the order of 0.075 μM.

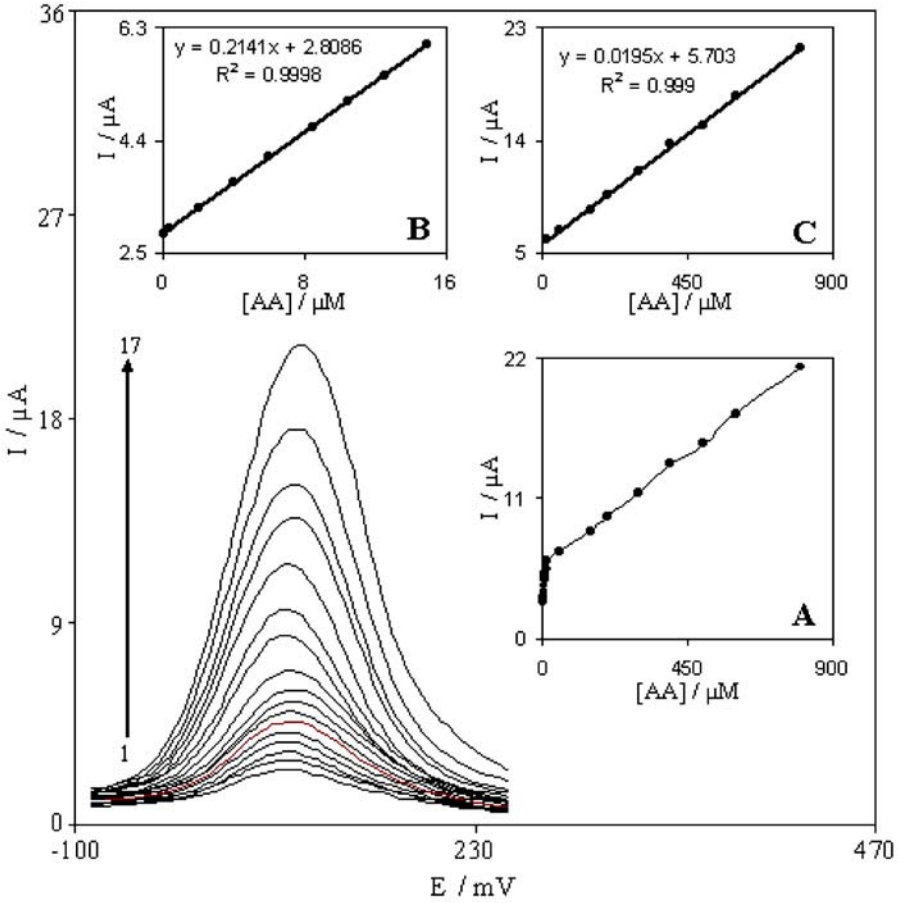


**Fig. 5** Differential pulse voltammograms of EBNBHCNPE in 0.1 M phosphate buffer solution (pH 7.0) containing different concentrations of AA. The numbers 1–17 correspond to 0.1, 0.4, 2, 4, 6, 8.5, 10.5, 12.5, 15, 50, 150, 200, 300, 400, 500, 600 and 800 μM of AA. Insets show the plots of the electrocatalytic peak current as a function of AA concentration in the range of *A* 0.1 to 800 μM, *B* 0.1 to 15 μM, and *C* 15 to 800 μM

## Simultaneous determination of ascorbic acid and uric acid

Because both AA and UA are oxidisable compounds, their detection can be made by electrochemical methods based on anodic oxidation. However, AA and UA are oxidized at nearly the same potential with poor sensitivity at solid unmodified electrodes. The use of chemically modified electrodes greatly increases the selectivity and sensitivity toward these analytes. DPV was used for the determination of AA and UA at the EBNBHCNP because of its higher current sensitivity and better resolution than cyclic voltammetry.

The determination of UA and AA in their mixtures was performed at the EBNBHCNPE when the concentration of UA changed, whereas the AA concentration remained constant. The peak current of UA is positively proportional to its concentration from 20–700 μM with sensitivity of 0.035 $\mu A.\mu M^{-1}$ when keeping the concentration of AA at 20 μM. No changes in the peak current and potential of AA can be found. Detection limit of UA was obtained 15 μM.

Also, as shown in Fig. 6, the oxidation peak current of AA and UA increases with increasing of the concentrations of two compounds AA and UA. Figure 6 insets A and B show the dependence of DPV peak currents on the concentration of AA and UA, respectively. The sensitivities of the modified electrode towards the oxidation of AA found to be 0.0195 $\mu A.\mu M^{-1}$, whereas the sensitivities towards AA in the absence of UA were found to be 0.0193 $\mu A.\mu M^{-1}$. It is very interesting to note that the sensitivities of the modified electrode towards AA in the absence and presence of UA are virtually the same, which indicates the fact that the oxidation processes of AA and UA at the EBNBHCNPE are independent and therefore simultaneous or independent measurements of the two analytes are possible without any interference. If the AA signal is affected by the UA, the above-mentioned slopes would be different.

## Rotating disk electrode voltammetry

To our knowledge, no paper has used Rotating disk electrode (RDE) voltammetry technique with carbon paste and specially carbon nanotube paste electrodes, and in this

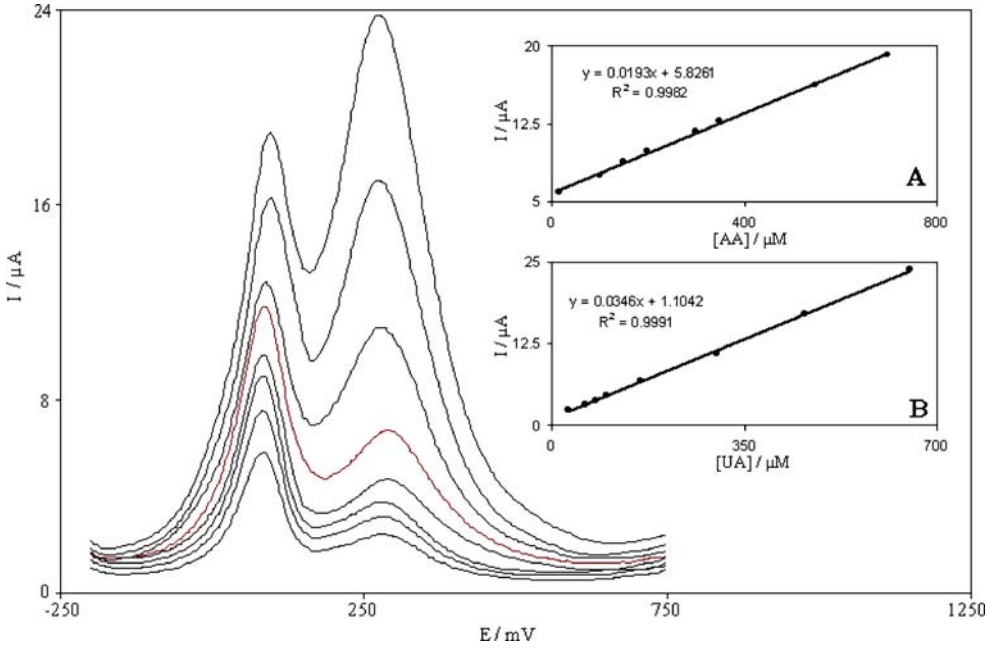


**Fig. 6** Differential pulse voltammograms of EBNBHCNPE in 0.1 M phosphate buffer solution (pH 7.0) containing different concentrations of AA and UA. (from inner to outer) mixed solutions of 15+30, 100+60, 150+80, 200+100, 300+160, 350+300, 550+460, and 700+650, respectively, in which the first value is concentration of AA in μM and the second value is concentration of UA in μM. Insets: *A* Plot of the peak currents as a function of AA concentration *B* Plot of the peak currents as a function of UA concentration

paper, we used this technique for the first time by this kind of electrodes. Thus, the electrocatalytic activity of EBNBHCNPE toward oxidation of AA was also evaluated by RDE voltammetry technique. The steady-state I–E curves were recorded for the oxidation of AA at EBNBHCNPE under various experimental conditions. In the case that the oxidation of AA at the surface EBNBHCNPE is controlled solely by the mass transfer process in the solution, the relationship between the limiting current and rotating speed should obey the Levich equation [33]

$$I_l = I_{Lev} = 0.620nFAD^{2/3}v^{-1/6}\omega^{1/2}C \quad (9)$$

where $D$, $v$, $\omega$ and $C$ are the diffusion coefficient, the kinematics viscosity, the rotation speed and the bulk concentration of the reactant in the solution, respectively, and all other parameters have their conventional meanings. Based on Eq. 9, the plot of limiting current $I_l$ as function of the $\omega^{1/2}$ should be a straight line. According to the Levich plots, the current increases with increasing electrode rotation speed, but were found to be nonlinear, including kinetic limitations. For irreversible reaction, relation between the limiting current and rotating speed has been given by Koutecky–Levich equation [33]:

$$[I_l]^{-1} = [nFACK\Gamma]^{-1} + [0.620nFAD^{2/3}v^{-1/6}C\omega^{1/2}]^{-1} \quad (10)$$

where $A$, $C$, $K$, $\Gamma$, $D$, $v$, and $\omega$ are the electrode area ($cm^2$), substrate concentration (mol $cm^{-3}$), catalytic rate constant ($cm^3$ $mol^{-1}s^{-1}$), surface coverage (mol $cm^{-2}$), diffusion coefficient ($cm^2$ $s^{-1}$), kinematics viscosity ($cm^2$ $s^{-1}$), and rotation speed (rad $s^{-1}$), respectively. It was seen that the intercepts of all linear plots are positive, clearly indicating the kinetic limitation of the electrode process. In addition, the slopes and intercepts were inversely proportional to the bulk concentration of AA, suggesting that the current is not limited by the rate of electron transport within the electrode. According to Eq. 10, the plot of $[I_l]^{-1}$ vs $\omega^{-1/2}$ gives a straight line. The rate-determining step must be catalytic process at electrode surface or electron diffusion process within the electrode. The value of the rate constant for the catalytic reaction $k$ can be obtained from the intercept of the Koutecky–Levich plot. The value of heterogeneous rate

**Table 2** Determination of ascorbic acid in real samples

| Pharmaceutical preparation | Claimed (mg) | Proposed method[a] (mg)(%RSD) | Iodine method[a] (mg; %RSD) | $F_{exp.}$ | $T_{exp.}$ |
|---|---|---|---|---|---|
| Effervescent tablet | 1,000 per tablet | 970.2 (0.3) | 965.8 (0.5) | 1.95 | 0.9 |
| Ampoule | 500 per 5 ml | 499.1 (0.5) | 501.5 (0.6) | 1.10 | 1.19 |
| Multivitamine syrup | 60 per 5 ml | 59.5 (1.5) | 60.3 (1.7) | 2.25 | 1.3 |

[a] Result based on five replicate determinations per samples. Theoretical values for $t$=2.31 and $F$=6.39 ($p$=0.05)

constant for EBNBHCNPE by using intercepts of the Koutecky–Levich was found to be $9.16\times10^{-4}$ $cms^{-1}$ for AA concentration in the range 1.0–9.0 mM. Diffusion coefficient of AA, D, may be obtained from the slope of Koutecky–Levich plots. The mean value of *D* was found to be $6.4\times10^{-6}$ $cm^2$ $s^{-1}$.

The repeatability and stability of EBNBHCNPE

The electrode capability for the generation of a reproducible surface was examined by cyclic voltammetric data obtained in optimum solution pH from five separately prepared EBNBHCNPEs. The calculated RSD for various parameters accepted as the criteria for a satisfactory surface reproducibility (1–4%). This degree of reproducibility is virtually the same as that expected for the renewal or ordinary carbon paste surface. In addition, the long-term stability of the EBNBHCNPE was tested over a 3-week period. When CVs were recorded after the modified electrode was stored in an atmosphere at room temperature, the peak potential for AA oxidation was unchanged, and the current signals showed only less than 2.0% decrease of the initial response. The antifouling properties of modified electrode toward AA oxidation and its oxidation products were investigated by recording the cyclic voltammograms of modified electrode before and after using in the presence of AA. Cyclic voltammograms were recorded in the presence of AA after having cycled the potential for 20 cycles at a scan rate 10 $mVs^{-1}$. The peak potentials were unchanged to positive values and the currents decreased by less than 2.1%. Therefore, at the surface of EBNBHCNPE, not only does the sensitivity increase, but the fouling effect of the analyte and its oxidation product also decreases. However, we regenerated the surface of EBNBHCNPE before each experiment.

Determination of ascorbic acid in pharmaceutical sample

The proposed EBNBHCNPE was found to work well under laboratory conditions. The electrode was also successfully applied to the direct determination of AA content of pharmaceutical samples. The AA content in pharmaceutical samples was determined by the standard addition method in order to prevent of any matrix effect. The results for the analysis of pharmaceutical samples with the voltammetric method compared favorably with those obtained by the USP standard method (Table 2).

## Conclusions

This work demonstrates the construction of a chemically modified carbon nanotube paste electrode by the incorporation of 2,2′-[1,2-ethanediylbis (nitriloethylidyne)]-bis-hydroquinone as modifying species. The value of the peak separation potential obtained for the 2,2′-[1,2-ethanediylbis (nitriloethylidyne)]-bis-hydroquinone/2,2′-[1, 2-ethanediylbis (nitriloethylidyne)]-bis-quinone couple suggests that the couple can act as quasi-reversible system in the carbon nanotube paste matrix. The carbon nanotube paste electrode modified with 2,2′-[1,2-ethanediylbis (nitriloethylidyne)]-bis-hydroquinone was considerably stable. Detection limit and potential shifts obtained by this electrode are better than values by other works (Table 1). This electrode is simple, easy to prepare and surface renewal is easy. The electrochemical behavior of the 2,2′-[1,2-ethanediylbis (nitriloethylidyne)]-bis-hydroquinone has been studied by cyclic voltammetry and chronoamperometry in both the absence and presence of AA. The results show that the oxidation of AA is catalyzed at pH 7.0, whereas the peak potential of AA is shifted by 380 mV to a less positive potential at the surface of the EBNBHCNPE. The EBNBHCNPE exhibits highly electrocatalytic activity to the oxidations of AA and UA. The modified electrode displays higher selectivity in voltammetric measurements of AA and UA in their mixture solution. The separations of the oxidation peak potentials for AA-UA are about 170 mV by differential pulse voltammetry.

**Acknowledgement** The authors wish to thankful the Yazd University Research Council, IUT Research Council, and Excellence in Sensors for financial support of this research.

## References

1. Markas AT, Hart JP (1995) Analyst 120:1029
2. Remita H, Siril PF, Mbomekalle IM, Keita B, Nadjo L (2006) J Solid State Electrochem 10:506
3. Goyal RN, Bachheti N, Tyagi A, Pandey AK (2007) Anal Chim Acta 605:34
4. Shamsipur M, Ershad S, Samadi N, Moghimi A, Aghabozorg H (2005) J Solid State Electrochem 9:788
5. Jin GP, Lin XQ (2004) Electrochem Commun 6:454
6. Zhang Y, Chen X, Yang W (2007) Sens Actuators B 130:682
7. Iijima S, Ichihashi T (1993) Nature 363:603
8. Ci L, Zhu H, Wei B, Xu C, Wu D (2003) Appl Surf Sci 205:39
9. Robinson JA, Snow ES, Perkins FK (2007) Sens Actuators A 135:309
10. Ng SH, Wang J, Guo ZP, Chen J, Wang GX, Liu HK (2005) Electrochim Acta 51:23
11. Saito Y, Hata K, Takakura A, Yotani J, Umemura S (2002) Physica B 323:30
12. Burini G (2007) J Chromatogr 1154:97
13. Kim WS, Dahlgren RL, Moroz LL, Sweedler JV (2002) Anal Chem 74:5614
14. Mohadesi A, Taher MA (2007) Sens Actuators B 123:733
15. Wang K, Xu J, Tang K, Chen H (2005) Talanta 67:798
16. Li NB, Ren W, Luo HQ, (2007) J Solid State Electrochem 12:693–699
17. Thangamuthu R, Senthil Kumar SM, Chandrasekara Pillai K (2007) Sens Actuators B 120:745

18. Raoof JB, Ojani R, Beitollahi H, Hosseinzadeh R (2006) Electroanalysis 18:1193
19. Wang S, Du D (2004) Sens Actuators B 97:373
20. Pournaghi-Azar MH, Ojani R (1999) J Solid State Electrochem 3:392
21. Tian L, Chen L, Liu L, Lu N, Song W, Xu H (2006) Sens Actuators B 113:150
22. Shakkthivel P, Chen SM (2007) Biosens Bioelectron 22:1680
23. Zhang L (2007) Electrochim Acta 52:6969
24. Ci L, Rao Z, Zhou Z, Tang D, Yan X, Liang Y (2002) Chem Phys Lett 359:63
25. Sugai T, Yoshida H, Shimada T, Okazaki T, Shinohara H, Bandow S (2003) Nano Lett 3:769
26. Okubo S, Sekine T, Suzuki S, Achiba Y, Tsukagoshi K, Aoyagi Y, Kataura H (2004) Jap J Appl Phys 43:L396
27. Igarashi H, Murakami H, Murakami Y, Maruyama S, Nakashima N (2004) Chem Phys Lett 392:529
28. Ramesh P, Okazaki T, Sugai T, Kimura J, Kishi N, Sato K, Ozeki Y, Shinohara H (2006) Phys Lett 418:408
29. Laviron E (1979) J Electroanal Chem 101:19
30. Bard AJ, Faulkner LR (2001) Electrochemical methods, fundamentals and applications. Wiley, New York
31. Andrieux CP, Saveant JM (1978) J Electroanal Chem 93:163
32. Galus Z (1976) Fundamentals of electrochemical analysis. Ellis Horwood, New York
33. Golabi SM, Noor-Mohammadi F (1998) J Solid State Electrochem 2:30